Molecular Vibrations and Force Fields of Alkyl Sulfides. VII. Polythiomethylene (PTM) and Polythiomethylene-d_2 (PTM-D2), and Their Model Compounds: $CH_3S(CH_2S)_nCH_3$ $(n=1—3)$

Masaru Ohsaku

Department of Chemistry, Faculty of Science, Hiroshima University, Higashisenda-machi, Hiroshima 730

(Received June 20, 1973)

Infrared spectra of polythiomethylene (PTM) and polythiomethylene-d_2 (PTM-D2) observed by a Nujol mull method are reported, and their spectra are assigned. Normal coordinates of bis(methylthio)methane, CH_3SCH_2-SCH_3, bis(methylthiomethyl) sulfide, $CH_3SCH_2SCH_2SCH_3$, bis[methylthio(methylthio)]methane, $CH_3SCH_2SCH_2$-SCH_2SCH_3, PTM, and PTM-D2 have been treated. The force field used in the computation is a modified Urey-Bradley type. The skeletal conformation of these model compounds in the solid state is confirmed to be the [G] form. The relations between the degree of n and their CH_2 deformation fundamentals are explained by the concept of the frequency-phase difference. The calculated frequencies are compared with those of experiment. A comparison of the force fields of PTM and polyoxymethylene (POM) is also briefly made.

Vibrational analyses[1-5] of the hexagonal polyoxymethylene (POM) and polyoxymethylene-d_2 (POM-D2), and those of their model compounds,[6,7] CH_3O-$(CH_2O)_nCH_3$ $(n=1—5)$, have been extensively treated. The X-ray analyses of the hexagonal POM have also been made.[8-11] For the sulfur analogs, in the first paper of this series[12] it has been described that the interaction terms on the methyl groups are indispensable in the force fields of dimethyl sulfide. In the second paper,[13] the analyses were made on the infrared spectra of this series: $CH_3S(CH_2S)_nCH_3$ $(n=0—3)$. These are model compounds of polythiomethylene (PTM). The preparation methods of PTM have been investigated.[14,15] An identification by means of the infrared spectra of PTM, which was obtained by the polymerization of s-trithiane, was very briefly made.[16] Recently, Hendra et al.[17] reported the Raman and infrared spectra of PTM and polyselenomethylene (PSeM). They also tentatively assigned the observed bands. However, no reports on normal coordinates of PTM have been published. The vibrational treatments of deuterated PTM (PTM-D2) have not been reported either. The molecular structure of the hexagonal PTM has already examined by Carazzolo and Val-

le by means of X-ray analysis,[10] as is shown in Fig. 1. The PTM is only known in the hexagonal form. They suggest that polymer chains are helicoidal, with the axis of the helix parallel to c, and that the unit cell is comprised of seventeen $-CH_2S-$ units and nine turns of the helix: $a=5.07$ Å, and $c=36.52$ Å. They have also estimated the internal rotation angle to be $65°59'$, i. e., the [G] form. The infrared spectra of PTM and its deuterated species, which were prepared according to the method of Ref. 14, have been recorded. Then, we tried to discuss the transferability of the set of the force constants obtained on dimethyl sulfide. Another purpose of this paper is to clarify the skeletal conformation of $CH_3S(CH_2S)_nCH_3$ $(n=1—3)$ in relation to the conformation of PTM. Still another purpose of this paper is to find the relations in the vibrational frequencies between PTM and POM. In the present paper, the molecular vibrations of the CH_3S-$(CH_2S)_nCH_3$ $(n=1—3)$, PTM, and PTM-D2 series are treated with a potential function of the modified Urey-Bradley type, assuming that all of the potential constants are common in this series.

Experimental

The preparation of PTM and PTM-D2 was done by the method of Schmidt et al.[14] The melting point of the purified PTM was 195—200 °C, while that of PTM-D2 was 175—180 °C. The infrared spectra were recorded by a Nujol mull method in the 4000—200 cm^{-1} region at room temperature.

Vibrational Assignment

The obtained infrared data are summarized in Table 1. The spectroscopically active vibrations of the hexagonal PTM or PTM-D2 are subdivided into A_1, A_2, and E species. Seven vibrations (the C–H or C–D stretching, methylene bending, twisting, C–S stretching, CSC bending, and the torsional vibrations) belong to the A_1 species. Five vibrations (the C–H or C–D stretching, methylene wagging, rocking, C–S stretching, and the torsional vibrations) belong to the A_2 species. Twelve degenerate vibrations belong to the E species. The vibrations belonging to the A_1 species are infrared-inactive. The vibrations of the A_2 and E species are
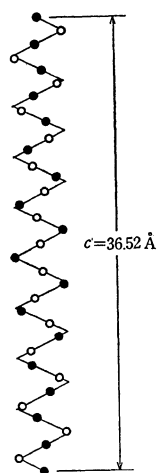

Fig. 1. Molecular structure of polythiomethylene (PTM) determined by the X-ray analysis.[10]
Open circle: methylene group. Closed circle: sulfur atom.

$c=36.52$ Å

Table 1. Infrared frequencies[a] (cm^{-1}), frequency
ratios, and assignments of polythiomethylene
(PTM) and polythiomethylene-d_2 (PTM-D2)

PTM[b]	PTM-D2[c]	ν_{PTM}/ν_{PTM-D2}	Assignment
1368 m	1012 m	1.352	CH_2, CD_2 bend
1225 vw	962 w	1.273	CH_2, CD_2 wag
1173 s	908 vs	1.292	CH_2, CD_2 wag
1155 sh, w	885 sh, w	1.305	CH_2, CD_2 twist
972 vvw	738 sh, vvw	1.32	—
946 vvw	675 sh, vvw	1.40	—
882 w	752 w	1.17	CH_2, CD_2 rock
742 w	635 sh, w	1.17	CH_2, CD_2 rock
735 m	697 m	1.05	C–S str
708 m	648 m	1.09	C–S str
671 w	603 w	1.11	C–S str
633 vw	585 sh, vw	1.08	—
511 vvvw	505 vvvw	1.01	—
467 vvvw	465 vvvw	1.00	—

s=strong, m=medium, w=weak, v=very, sh=shoulder.
a) Obtained in a Nujol mull. b) The region above
1400 cm^{-1} is omitted. c) The region above 1100 cm^{-1}
is omitted.

Table 2. Symmetry properties of PTM

Mode	A_1	A_2	E
νC–H	1	1	2
BCH$_2$	1	—	1
WCH$_2$	—	1	1
TCH$_2$	1	—	1
RCH$_2$	—	1	1
νC–S	1	1	2
BSCS	1	—	1
BCSC	1	—	1
τC–S	1	1	2
Infrared	inactive	//	⊥

ν, stretching; B, bending; W, wagging; T, twisting;
R, rocking; τ, torsion.

infrared-active. Table 2 shows the numbers of the
bands and the band types. The following bands may,
then, be expected in our spectral region: one methyl-
ene bending, two wagging, one twisting, two rocking,
three C–S stretching, and one skeletal bending vibra-
tions. The numbers of the obtained bands corres-
pond well with those expected.

Polythiomethylene. The spectra of PTM ob-
tained are closely similar to those of polymethylene
disulfide.[18] The spectra are virtually identical with
those of Hendra *et al.*[17] As for the CH_2 deformation
modes, the bands of the CH_2 bending, wagging, twisting,
and rocking are expected in the 1400—740 cm^{-1} region.
Hendra *et al.* did not completely assign the infrared
bands obtained in this region. In the 1400—1100
cm^{-1} region, one CH_2 bending, two wagging, and one
twisting bands may appear. The band at 1225 cm^{-1}
is assignable to the CH_2 wagging vibration. This
band, however, might be due to the other vibration.
The result of the normal-coordinates fairly well re-
produced this frequency. Although the CH_2 twist-

ing band is expected around 1150 cm^{-1}, no effec-
tively sharp bands appear around this region. There,
the weak shoulder band around 1150 cm^{-1} may be
identified to the CH_2 twisting vibration. To the
CH_2 rocking vibrations, two bands, at 882 and 742
cm^{-1}, were assigned. To the C–S stretching vibra-
tions, three bands at 735, 708, and 671 cm^{-1} are as-
signable. The bands at 742 and 735 cm^{-1} are very
close to each other. These vibrations of the bands may
be strongly coupled. Therefore, the assignments of
these bands are ambiguous. Hendra *et al.*[17] did not
assign the band at 742 cm^{-1} (their value—738 cm^{-1})
to any vibrational mode. They assigned the bands at
748 and 739 cm^{-1}, observed from the Raman spectra,
to the C–S stretching vibrations belonging to the E_2
species, though. In the skeletal deformation region,
below 400 cm^{-1}, none of the sharp bands appear. The
extremely weak band at 511 cm^{-1} may be due to the
vibration of the S–S bond. In that case, the PTM
obtained is not completely constructed by the head-to-
tail combination.

Polythiomethylene-d_2. Most of the bands of the
fully-deuterated PTM shift to a frequency region lower
than those of the normal species. To assign the bands,
it is useful to ascertain the frequency ratios of $\nu_{PTM}/$
ν_{PTM-D2}. The CD_2 deformation band is conspicuous
in the frequency shift. The band at 1012 cm^{-1} was
assigned to the CD_2 bending vibration. The bands at
962 and 908 cm^{-1}, and the shoulder band at 885 cm^{-1}
were assigned to the CD_2 wagging and twisting vibra-
tions. In the 700—550 cm^{-1} region, the obtained spectra
are more complicated than those of the normal species.
Although, in this region, we can expect the CD_2 rock-
ing and C–S stretching bands, each assignment is
difficult since the vibrations may be strongly coupled
with each other. In conclusion, we have assigned the
fairly strong bands to the C–S stretching vibrations.

Normal Coordinate Treatment

In order to confirm the previous assignments, the
normal coordinates, including all of the vibrational
degrees of freedom, were treated for the $n=1$—3 species
using a force function of the modified Urey-Bradley
type. The force constants in relation to the methyl
group were transferred from those of dimethyl sulfide,[12]
while the other constants were referred to those of 1,2-
ethanedithiol,[19] polymethylene disulfide,[18] and (meth-
ylthio)methanethiol.[20] The molecular parameters
used in the computations were: r(C–H)=1.09 Å,
r(C–S)=1.81 Å, and ϕ(CSC)=99°; the other bond
angles were assumed to be tetrahedral. The correc-
tion terms used were p, p', n, t, g, t', g', and l. The
corrections of p, p', n, t, g, and l have been explained in
a previous paper.[20] Additional terms, t' and g', which
were the *trans* and *gauche* coupling constants between
the HCS and CSC angles in the methylene group,
were introduced in order to explain the separation
width of the CH_2 deformation bands. The force con-
stants used in the computations are summarized in
Table 3. The diagonal elements of the potential
energy matrix, F, are also listed in Table 4. The
calculated frequencies are listed in Tables 5—7, toge-

TABLE 3. MODIFIED UREY-BRADLEY FORCE CONSTANTS[a]

K(C–H)	4.250[b]	CH_3 and CH_2 groups
K(C–S)	1.691[b]	CH_3–S and S–CH_2 bond
H(HCS)	0.030	CH_3 group
H(HCH)	0.366	CH_3 group
H(CSC)	0.244[b]	CH_3–S–CH_2 and CH_2–S–CH_2 angles
H(SCS)	0.150[b]	S–CH_2–S angle
H(SCH)	0.160[b]	CH_2 group
H(HCH)	0.335[b]	CH_2 group
F(HCS)	0.763	
F(HCH)	0.200	
F(CSC)	0.210[b]	
F(SCS)	0.500[b]	
F(SCH)	0.390[b]	
F(HCH)	0.200[b]	
κ	0.060	CH_3 group
	−0.010[b]	CH_2 group
Y	0.054[b]	CH_3–S and S–CH_2 bonds
p	−0.115[b]	CH_3 and CH_2 groups
p'	−0.100[b]	CH_3–S and S–CH_2 bonds
n	0.033	CH_3 group ($\angle$HCS and $\angle$HCH)
t	0.070	CH_3 group ($\angle$HCS and $\angle$CSC, trans)
g	−0.050	CH_3 group ($\angle$HCS and $\angle$CSC, gauche)
t'	0.100[b]	CH_2 group ($\angle$HCS and $\angle$CSC, trans)
g'	−0.040[b]	CH_2 group ($\angle$HCS and $\angle$CSC, gauche)
l	−0.005[b]	S–CH_2–S

a) Unit of K, H, F, p, and p' is in mdyn/Å; κ, Y, n, t, g, t', g', and l is in mdyn·Å; $F' = -0.1F$.　b) These constants are also used in polymers.

TABLE 4. DIAGONAL ELEMENTS[a] OF THE POTENTIAL ENERGY MATRIX (F)

4.843	CH_3 stretching
4.724	CH_2 stretching
3.632	CH_3–S stretching
2.743	S–CH_2 stretching
0.675	CH_3 group, HCS bending
0.594	CH_3 group, HCH bending
1.129	CH_3–S–CH_2 and CH_2–S–CH_2 bending
1.136	S–CH_2–S bending
0.582	CH_2 group, SCH bending
0.482	CH_2 group, HCH bending
0.054	CH_3–S and S–CH_2 bonds, internal rotation

a) Element of the stretching is in mdyn/Å; element of the bending or internal rotation is in mdyn·Å.

ther with the experimental frequencies.

In order to confirm the transferability of the force constants, the normal coordinates of PTM and PTM-D2 were also treated with the common force field of the model compounds. Calculations were made according to the analogous method of Tadokoro et al.[1] The molecular parameters used were: r(C–H)=1.09 Å, r(C–S)=1.815 Å, ϕ(CSC) and ϕ(SCS)=106°52′, and

ϕ(HCH)=109°28′, and the internal rotation angle was assumed to be 65°59′.

Molecular Forms. At first we will try to determine the stable conformation which exists in the solid state of the series of $n=1-3$. For the molecule of $n=1$, four forms are possible: TT, TG, GG, and GG′. For the $n=2$ and 3 species, a large number of forms are possible. In this treatment, however, we took into consideration the six most probable forms of TTTT, GGGG, TGTG, TTGT, TGGT, and TTGG for the $n=2$ species and of TTTTTT, GGGGGG, TGTGTG, TTGTTG, TGGTGG, and TTGGTT for the $n=3$ species. The calculated frequencies of the CH_2 rocking, C–S stretching, and skeletal deformation are fairly much affected by their internal angles. The observed frequencies are taken from the previous paper.[13] In the previous paper, however, more bands than those expected for one form are described in the 400—200 cm^{-1} region, even in the solid state. The bands of this region are essentially weak. Moreover, the reliability of the spectrophotometer is not very good in this region. Still another difficulty is due to the bands of water vapor in the atmosphere. A few of the bands which decrease in intensity in the solid state may be due to the imperfect annealing. Figure 2 shows the observed and calculated frequencies in relation to the skeletal vibrations through the $n=1-3$ species. On the molecule of $n=1$ the bands at 341 and 314 cm^{-1} are obviously due to the stable form in the solid state. The frequencies calculated for the GG form explain these bands well. On the species of $n=2$, the three bands at 339, 318, and 247 cm^{-1} can be assigned to the stable form in the solid state. These bands fit well to the frequencies calculated for the [G] form. In the same way, the calculated frequencies of the [G]
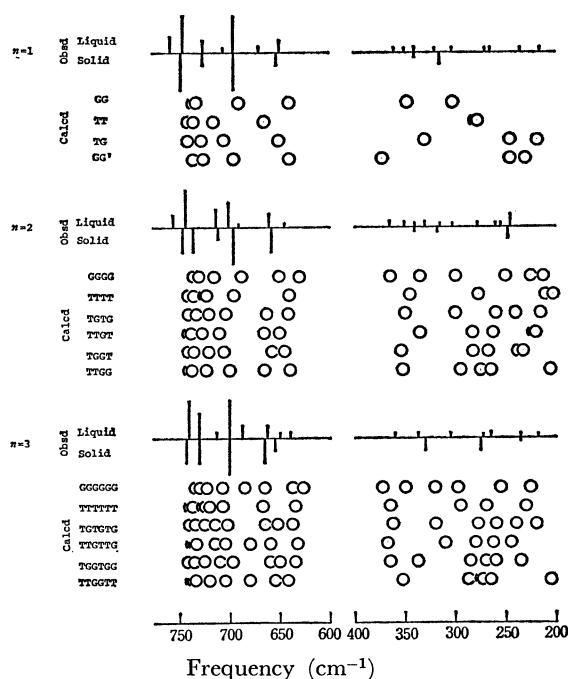

Fig. 2. Observed frequencies and relative intensities, and calculated frequencies of $CH_3S(CH_2S)_nCH_3$ ($n=1-3$) in relation to the skeletal vibrations.

TABLE 5. OBSERVED AND CALCULATED FREQUENCIES (cm^{-1}), AND POTENTIAL ENERGY

DISTRIBUTION, PED,[a] OF BIS(METHYLTHIO)METHANE

Obsd[b]	Calcd							
	GG	PED	TT[c]	PED	TG	PED	GG'	PED
1441_a	1441	ACH$_3$	1441	ACH$_3$	1441	ACH$_3$	1441	ACH$_3$
1436_a	1441	ACH$_3$	1441	ACH$_3$	1441	ACH$_3$	1441	ACH$_3$
1421_a	1441	ACH$_3$	1441	ACH$_3$	1441	ACH$_3$	1441	ACH$_3$
1417_a	1441	ACH$_3$	(1441)	ACH$_3$	1441	ACH$_3$	1441	ACH$_3$
1387_1	1388	BCH$_2$	1391	BCH$_2$	1390	BCH$_2$	1388	BCH$_2$
1327_1	1317	ΣCH$_3$	1317	ΣCH$_3$	1317	ΣCH$_3$	1317	ΣCH$_3$
1318_1	1317	ΣCH$_3$	1317	ΣCH$_3$	1317	ΣCH$_3$	1317	ΣCH$_3$
1203_1	1206	WCH$_2$	1204	WCH$_2$	1205	WCH$_2$	1206	WCH$_2$
(1163_1)			(1143)	TCH$_2$	1144	TCH$_2$	1145	TCH$_2$
1155_1	1146	TCH$_2$						
(1124_1)				—				
986_1	994	RCH$_3$	991	RCH$_3$	990	RCH$_3$	990	RCH$_3$
986_1	986	RCH$_3$	986	RCH$_3$	988	RCH$_3$	989	RCH$_3$
959_1	967	RCH$_3$	968	RCH$_3$	967	RCH$_3$	968	RCH$_3$
959_1	967	RCH$_3$	(967)	RCH$_3$	967	RCH$_3$	967	RCH$_3$
874_1				—				
(824_1)					802	RCH$_2$		
806_1	817	RCH$_2$					800	RCH$_2$
—			780	RCH$_2$				
(758_1)			739	νC–S	739	νC–S	736	νC–S
746_1	733	νC–S	735	νC–S				
724_1	733	νC–S			728	νC–S	723	νC–S
(705_1)			715	νC–S	704	νC–S		
694_1	690	νC–S					695	νC–S
(669_1)			665	νC–S, BSCS				
649_1	639	νC–S, BSCS			651	νC–S, BSCS	640	νC–S, BSCS
(360_1)							372	BCSC
(350_1)					331	BCSC, BSCS		
340_1	347	BSCS, BCSC						
321_1	302	BCSC						
303_1				—				
(270_1)			279	BCSC				
(265_1)			277	BSCS, τC–S				
235_1*					245	BCSC	245	BSCS, BCSC, τC–S
216_1*					218	BSCS, BCSC, τC–S	228	BCSC
—	189	BCSC, τC–S, BSCS						
—			(182)	τC–S				
—	174	τC–S	173	τC–S	175	τC–S	173	τC–S
—	162	τC–S, BSCS	170	BCSC, BSCS	165	τC–S	164	τC–S
—	79	τC–S	(75)	τC–S	71	τC–S		
—			65	τC–S			65	τC–S
—					55	τC–S		
—	44	τC–S					48	τC–S

ν, stretching; A, degenerate deformation; Σ, symmetrical deformation; B, bending; W, wagging; T, twisting; R, rocking; τ, torsion. The region above 1500 cm^{-1} is omitted. a) Only the predominant modes are shown. b) From Ref. 13. Figures in parentheses show the bands which disappear in the solid state. a, annealed- and l, liquid-state bands. *See text. c) A$_2$ species in parentheses.

TABLE 6. OBSERVED AND CALCULATED FREQUENCIES (cm^{-1}), AND POTENTIAL ENERGY DISTRIBUTION, PED OF BIS(METHYLTHIOMETHYL) SULFIDE

Obsd	GGGG	PED	TTTT	PED	TGTG	PED	TTGT	PED	TGGT	PED	TTGG	PED
1439_a	1441	ΔCH_3	1441	ΔCH_3	1442	ΔCH_3	1441	ΔCH_3	1442	ΔCH_3	1441	ΔCH_3
1434_a	1441	ΔCH_3	1441	ΔCH_3	1441	ΔCH_3	1441	ΔCH_3	1441	ΔCH_3	1441	ΔCH_3
1416_a	1441	ΔCH_3	1441	ΔCH_3	1441	ΔCH_3	1441	ΔCH_3	1441	ΔCH_3	1441	ΔCH_3
1410_a	1441	ΔCH_3	(1441)	ΔCH_3	1441	ΔCH_3	1441	ΔCH_3	1441	ΔCH_3	1441	ΔCH_3
1395_1	1389	BCH_2	1392	BCH_2	1390	BCH_2	1391	BCH_2	1390	BCH_2	1391	BCH_2
1379_1	1388	BCH_2	1389	BCH_2	1389	BCH_2	1390	BCH_2	1389	BCH_2	1389	BCH_2
1327_1	1317	$\sum CH_3$	1317	$\sum CH_3$	1317	$\sum CH_3$	1317	$\sum CH_3$	1317	$\sum CH_3$	1317	$\sum CH_3$
1317_1	1317	$\sum CH_3$	1317	$\sum CH_3$	1317	$\sum CH_3$	1317	$\sum CH_3$	1317	$\sum CH_3$	1317	$\sum CH_3$
1218_1	1206	WCH_2	1206	WCH_2	1207	WCH_2	1206	WCH_2	1206	WCH_2	1206	WCH_2
1193_1	1206	WCH_2	1203	WCH_2	1204	WCH_2	1204	WCH_2	1205	WCH_2	1204	WCH_2
1165_1	1148	TCH_2	1145	TCH_2	1149	TCH_2	1148	TCH_2	1149	TCH_2	1150	TCH_2
1132_1	1147	TCH_2	(1141)	TCH_2	1145	TCH_2	1141	TCH_2	1143	TCH_2	1144	TCH_2
(1119_1)							——					
974_1	991	RCH_3	989	RCH_3	990	RCH_3	989	RCH_3	989	RCH_3	990	RCH_3
974_1	990	RCH_3	989	RCH_3	989	RCH_3	989	RCH_3	989	RCH_3	989	RCH_3
961_1	968	RCH_3	967	RCH_3	968	RCH_3	968	RCH_3	968	RCH_3	968	RCH_3
961_1	967	RCH_3	(967)	RCH_3	967	RCH_3	967	RCH_3	968	RCH_3	968	RCH_3
(855_1)									830	RCH_2		
841_1	839	RCH_2										
(834_1)											826	RCH_2
(820_1)					815	RCH_2	808	RCH_2				
778_1	796	RCH_2	788	RCH_2	795	RCH_2	790	RCH_2	791	RCH_2	797	RCH_2
—			(775)	RCH_2								
(754_1)			741	νC–S	740	νC–S	739	νC–S	739	νC–S	738	νC–S
742_1	736	νC–S	734	νC–S	733	νC–S	737	νC–S	734	νC–S	736	νC–S
742_1	730	νC–S	723	νC–S			727	νC–S	721	νC–S	723	νC–S
712_1	716	νC–S	722	νC–S	719	νC–S	711	νC–S	706	νC–S		
700_1	688	νC–S	694	νC–S, BSCS, BCSC	703	νC–S					699	νC–S
(690_1)							667	νC–S, BSCS			667	νC–S, BSCS
661_1	649	νC–S, BSCS			662	νC–S, BSCS	649	νC–S, BSCS	657	νC–S, BSCS		
(645_1)	630	νC–S, BSCS	642	νC–S	642	νC–S, BSCS			647	νC–S, BSCS	640	νC–S, BSCS
(365_1)	364	BCSC, BSCS										
(350_1)			345	BSCS, BCSC	351	BSCS, BCSC, νC–S			353	BCSC, BSCS	352	BSCS, BCSC
(340_1)							336	BSCS, BCSC, νC–S				
331_1	331	BCSC, BSCS										
315_1	299	BCSC										
(305_1)					299	BSCS					294	BCSC
277_1*			278	BCSC			283	BCSC, BSCS	282	BSCS, νC–S	274	BCSC, BSCS, νC–S
(259_1)							263	τC–S	268	τC–S	266	τC–S
(254_1)					259	τC–S						
244_1	250	τC–S, BCSC			239	BCSC, BSCS			237	BCSC, BSCS		
—	225	τC–S					222	BCSC	233	BCSC		
—	213	BSCS, τC–S, BCSC	209	BCSC, BSCS	215	BCSC, τC–S	218	BSCS, BCSC				
—			202	BSCS, νC–S, BCSC	190	BCSC, τC–S, BSCS			195	τC–S	206	BSCS, BCSC
—			179	τC–S	179	τC–S, BCSC, BSCS						
—			(177)	τC–S			173	BCSC, τC–S, BSCS	172	BSCS, BCSC, τC–S		
—											145	BCSC, τC–S, BSCS
—					143	τC–S					143	τC–S

Tᴀʙʟᴇ 6. Cᴏɴᴛɪɴᴜᴇᴅ

Obsd	Calcd										
	GGGG	PED	TTTT	PED	TGTG	PED	TTGT	PED	TGGT	PED	TTGG	PED
—	131	BSCS, BCSC										
—							107	τC–S	107	τC–S	114	τC–S
—	99	τC–S	98	τC–S								
—			92	BCSC, BSCS								
—			(82)	τC–S	77	τC–S						
—	63	τC–S			67	τC–S	68	τC–S	71	τC–S	72	τC–S
—									62	τC–S	59	τC–S
—	46	τC–S	48	τC–S	52	τC–S	47	τC–S				
—			(38)	τC–S			42	τC–S				
—	28	τC–S			34	τC–S			32	τC–S		
—											22	τC–S

Notations are the same as in Table 5.

Tᴀʙʟᴇ 7. Oʙsᴇʀᴠᴇᴅ ᴀɴᴅ ᴄᴀʟᴄᴜʟᴀᴛᴇᴅ ꜰʀᴇǫᴜᴇɴᴄɪᴇs (cm^{-1}), ᴀɴᴅ ᴘᴏᴛᴇɴᴛɪᴀʟ ᴇɴᴇʀɢʏ ᴅɪsᴛʀɪʙᴜᴛɪᴏɴ, PED, ᴏꜰ ʙɪs[(ᴍᴇᴛʜʏʟᴛʜɪᴏ)ᴍᴇᴛʜʏʟᴛʜɪᴏ]ᴍᴇᴛʜᴀɴᴇ

Obsd	Calcd										
	GGGGGG	PED	TTTTTT	PED	TGTGTG	PED	TTGTTG	PED	TGGTGG	PED	TTGGTT	PED
1446_a	1442	$\varDelta\mathrm{CH}_3$	1441	$\varDelta\mathrm{CH}_3$	1441	$\varDelta\mathrm{CH}_3$	1441	$\varDelta\mathrm{CH}_3$	1441	$\varDelta\mathrm{CH}_3$	1441	$\varDelta\mathrm{CH}_3$
1441_a	1441	$\varDelta\mathrm{CH}_3$	1441	$\varDelta\mathrm{CH}_3$	1441	$\varDelta\mathrm{CH}_3$	1441	$\varDelta\mathrm{CH}_3$	1441	$\varDelta\mathrm{CH}_3$	1441	$\varDelta\mathrm{CH}_3$
1431_a	1441	$\varDelta\mathrm{CH}_3$	1441	$\varDelta\mathrm{CH}_3$	1441	$\varDelta\mathrm{CH}_3$	1441	$\varDelta\mathrm{CH}_3$	1441	$\varDelta\mathrm{CH}_3$	1441	$\varDelta\mathrm{CH}_3$
1418_a	1441	$\varDelta\mathrm{CH}_3$	(1441)	$\varDelta\mathrm{CH}_3$	1441	$\varDelta\mathrm{CH}_3$	1441	$\varDelta\mathrm{CH}_3$	1441	$\varDelta\mathrm{CH}_3$	1441	$\varDelta\mathrm{CH}_3$
(1401_1)							——					
1394_1	1389	$B\mathrm{CH}_2$	1393	$B\mathrm{CH}_2$	1390	$B\mathrm{CH}_2$	1391	$B\mathrm{CH}_2$	1390	$B\mathrm{CH}_2$	1391	$B\mathrm{CH}_2$
1378_1	1388	$B\mathrm{CH}_2$	1391	$B\mathrm{CH}_2$	1390	$B\mathrm{CH}_2$	1391	$B\mathrm{CH}_2$	1389	$B\mathrm{CH}_2$	1391	$B\mathrm{CH}_2$
1378_1	1388	$B\mathrm{CH}_2$	1389	$B\mathrm{CH}_2$	1389	$B\mathrm{CH}_2$	1389	$B\mathrm{CH}_2$	1388	$B\mathrm{CH}_2$	1389	$B\mathrm{CH}_2$
1316_1	1317	$\Sigma\mathrm{CH}_3$	1317	$\Sigma\mathrm{CH}_3$	1317	$\Sigma\mathrm{CH}_3$	1317	$\Sigma\mathrm{CH}_3$	1317	$\Sigma\mathrm{CH}_3$	1317	$\Sigma\mathrm{CH}_3$
1316_1	1317	$\Sigma\mathrm{CH}_3$	1317	$\Sigma\mathrm{CH}_3$	1317	$\Sigma\mathrm{CH}_3$	1317	$\Sigma\mathrm{CH}_3$	1317	$\Sigma\mathrm{CH}_3$	1317	$\Sigma\mathrm{CH}_3$
1223_1	1206	$W\mathrm{CH}_2$	1206	$W\mathrm{CH}_2$	1207	$W\mathrm{CH}_2$	1207	$W\mathrm{CH}_2$	1207	$W\mathrm{CH}_2$	1207	$W\mathrm{CH}_2$
(1205_1)			1204	$W\mathrm{CH}_2$	1206	$W\mathrm{CH}_2$	1205	$W\mathrm{CH}_2$	1205	$W\mathrm{CH}_2$	1205	$W\mathrm{CH}_2$
1199_1	1206	$W\mathrm{CH}_2$										
1188_1	1206	$W\mathrm{CH}_2$	1202	$W\mathrm{CH}_2$	1204	$W\mathrm{CH}_2$	1203	$W\mathrm{CH}_2$	1205	$W\mathrm{CH}_2$	1204	$W\mathrm{CH}_2$
1171_1	1148	$T\mathrm{CH}_2$	(1146)	$T\mathrm{CH}_2$	1149	$T\mathrm{CH}_2$	1149	$T\mathrm{CH}_2$	1149	$T\mathrm{CH}_2$	1150	$T\mathrm{CH}_2$
1145_1	1148	$T\mathrm{CH}_2$	1143	$T\mathrm{CH}_2$	1146	$T\mathrm{CH}_2$	1145	$T\mathrm{CH}_2$	1145	$T\mathrm{CH}_2$	1146	$T\mathrm{CH}_2$
1125_1	1147	$T\mathrm{CH}_2$	(1140)	$T\mathrm{CH}_2$	1142	$T\mathrm{CH}_2$	1139	$T\mathrm{CH}_2$	1141	$T\mathrm{CH}_2$	1141	$T\mathrm{CH}_2$
971_1	991	$R\mathrm{CH}_3$	989	$R\mathrm{CH}_3$	990	$R\mathrm{CH}_3$	990	$R\mathrm{CH}_3$	990	$R\mathrm{CH}_3$	989	$R\mathrm{CH}_3$
971_1	990	$R\mathrm{CH}_3$	989	$R\mathrm{CH}_3$	989	$R\mathrm{CH}_3$	989	$R\mathrm{CH}_3$	989	$R\mathrm{CH}_3$	989	$R\mathrm{CH}_3$
960_1	968	$R\mathrm{CH}_3$	(967)	$R\mathrm{CH}_3$	968	$R\mathrm{CH}_3$	968	$R\mathrm{CH}_3$	968	$R\mathrm{CH}_3$	968	$R\mathrm{CH}_3$
960_1	967	$R\mathrm{CH}_3$	967	$R\mathrm{CH}_3$	967	$R\mathrm{CH}_3$	967	$R\mathrm{CH}_3$	967	$R\mathrm{CH}_3$	967	$R\mathrm{CH}_3$
858_1	849	$R\mathrm{CH}_2$							833	$R\mathrm{CH}_2$	831	$R\mathrm{CH}_2$
820_1	816	$R\mathrm{CH}_2$			818	$R\mathrm{CH}_2$	810	$R\mathrm{CH}_2$	822	$R\mathrm{CH}_2$		
(785_1)			791	$R\mathrm{CH}_2$	804	$R\mathrm{CH}_2$	800	$R\mathrm{CH}_2$			798	$R\mathrm{CH}_2$
763_1	788	$R\mathrm{CH}_2$	(782)	$R\mathrm{CH}_2$	788	$R\mathrm{CH}_2$	790	$R\mathrm{CH}_2$	788	$R\mathrm{CH}_2$	783	$R\mathrm{CH}_2$
763_1			773	$R\mathrm{CH}_2$								
740_1	735	νC–S	740	νC–S	740	νC–S	738	νC–S	739	νC–S	737	νC–S
740_1	731	νC–S	737	νC–S	735	νC–S	737	νC–S	735	νC–S	737	νC–S
731_1	722	νC–S	727	νC–S	726	νC–S	731	νC–S	724	νC–S	732	νC–S
731_1			726	νC–S							721	νC–S .
(712_1)			719	νC–S	714	νC–S	714	νC–S	710	νC–S		
700_1	708	νC–S	707	νC–S, BCSC, BSCS	702	νC–S	705	νC–S	698	νC–S	704	νC–S
(687_1)	687	νC–S					680	νC–S, BSCS			680	νC–S, BSCS
663_1	665	νC–S, BSCS	667	νC–S, BSCS	666	νC–S, BSCS	661	νC–S, BSCS	661	νC–S, BSCS	656	νC–S, BSCS
651_1	637	νC–S, BSCS			653	νC–S, BSCS			651	νC–S, BSCS		
(640_1)	627	νC–S, BSCS	636	νC–S	638	νC–S, BSCS	633	νC–S	636	νC–S, BSCS	643	νC–S, BSCS

TABLE 7. CONTINUED

Obsd	GGGGGG	PED	TTTTTT	PED	TGTGTG	PED	TTGTTG	PED	TGGTGG	PED	TTGGTT	PED
(360_1)	372	$BSCS, BCSC$	366	$BSCS, BCSC$	362	$BSCS, BCSC, \nu C\text{-}S$	368	$BSCS, BCSC$	364	$BSCS, BCSC$	353	$BSCS, BCSC$
338_1	349	$BCSC, BSCS$							337	$BCSC, BSCS$		
338_1	320	$BCSC, BSCS$			319	$BCSC, BSCS$						
(305_1)	297	$BCSC$	295	$BSCS, BCSC, \nu C\text{-}S$			310	$BCSC, BSCS, \nu C\text{-}S$				
272_1					277	$BSCS, BCSC$	281	$BCSC, BSCS$	286	$BCSC$	288	$BCSC$
272_1	256	$BSCS, BCSC$	271	$BCSC$					271	$\tau C\text{-}S$	275	$BSCS, \nu C\text{-}S, BCSC$
272_1											273	$BCSC, BSCS$
265_1					259	$\tau C\text{-}S$	263	$\tau C\text{-}S$	260	$BSCS, \tau C\text{-}S$	266	$\tau C\text{-}S$
235_1	227	$\tau C\text{-}S$	231	$BCSC, BSCS$	239	$BCSC$	244	$BCSC, BSCS$	234	$BCSC$		
217_1*					221	$BCSC, BSCS, \tau C\text{-}S$					205	$BSCS, BCSC$
—	191	$BSCS, BCSC$			188	$BSCS, BCSC, \tau C\text{-}S$	194	$BSCS, BCSC$			194	$BCSC, BSCS$
—			(178)	$\tau C\text{-}S$	185	$BCSC, \tau C\text{-}S, BSCS$			181	$BSCS, BCSC$	189	$\tau C\text{-}S$
—			178	$\tau C\text{-}S$			176	$\tau C\text{-}S \ BCSC$				
—	162	$\tau C\text{-}S$	160	$BSCS, \nu C\text{-}S, BCSC$	164	$\tau C\text{-}S$	166	$BCSC, \tau C\text{-}S, BSCS$	157	$BCSC, BSCS, \tau C\text{-}S$		
—									148	$\tau C\text{-}S$		
—			139	$BCSC, BSCS$			136	$BSCS, BCSC, \tau C\text{-}S$				
—	110	$\tau C\text{-}S$									119	$\tau C\text{-}S$
—	104	$BCSC, BSCS$	(109)	$\tau C\text{-}S$			107	$\tau C\text{-}S$	113	$\tau C\text{-}S$	104	$BCSC, \tau C\text{-}S, BSCS$
—			91	$\tau C\text{-}S$							86	$\tau C\text{-}S$
—	76	$\tau C\text{-}S$	(70)	$\tau C\text{-}S$	78	$\tau C\text{-}S$	78	$\tau C\text{-}S$	72	$\tau C\text{-}S$	71	$\tau C\text{-}S$
—					73	$\tau C\text{-}S$	67	$\tau C\text{-}S$	65	$\tau C\text{-}S$		
—			58	$\tau C\text{-}S$	60	$\tau C\text{-}S$						
—	50	$\tau C\text{-}S$	56	$BCSC, BSCS$			54	$\tau C\text{-}S$			51	$\tau C\text{-}S$
—			36	$\tau C\text{-}S$	42	$\tau C\text{-}S$			38	$\tau C\text{-}S$	41	$\tau C\text{-}S$
—	30	$\tau C\text{-}S$	(25)	$\tau C\text{-}S$	27	$\tau C\text{-}S$	30	$\tau C\text{-}S$				
—	25	$\tau C\text{-}S$			22	$\tau C\text{-}S$	22	$\tau C\text{-}S$	22	$\tau C\text{-}S$		
—	23	$\tau C\text{-}S$							21	$\tau C\text{-}S$		
—											12	$\tau C\text{-}S$

Notations are the same as in Table 5.

form explain well the bands which are observed in the solid state of the $n=3$ species. Therefore, it is likely that these three molecules stay in the [G] form in the solid state. In the C–S stretching region, the calculated frequencies of the [G] form fit the observed frequencies well.

The molecular conformations existing in the liquid state will now be briefly described. We will first consider the molecular species of $n=1$. In the region below 400 cm⁻¹, which was observed in the liquid state, there are bands which correspond to at least three forms. In a previous paper,[13] the GG' form was excluded from the stable forms. In Table 5, however, the frequencies calculated for the GG' form are listed for reference. The GG form, which is the stable form in the solid state, was also excluded from consideration in this section. Two forms then remain: TT and TG. In the C–S stretching region, the band at 758 cm⁻¹ observed in the liquid state fits fairly well to the frequencies

calculated for the TT and/or TG form. The band at 705 cm⁻¹ fits well to the frequencies calculated for the TT and/or TG form. The weak band at 669 cm⁻¹ fits well to the frequency calculated for the TT form. In the skeletal deformation region, nine bands appear in the liquid state. Two bands which disappear in the unannealed film were excluded from the fundamentals, since, around this region, there are not the corresponding calculated frequencies, although these bands may be due to the GG' form. Four bands then remain at 270, 260, 235, and 220 cm⁻¹. Among these bands, the two bands at 270 and 260 cm⁻¹ fit well to the frequencies calculated for the TT form, while the bands at 235 and 220 cm⁻¹ fit well to the frequencies calculated for the TG form. Therefore, it may be concluded that three conformations, TT, TG, and GG, coexist in the liquid or gaseous state for the $n=1$ species. Moreover, the following descriptions can be postulated. The bands at 235 and

220 cm⁻¹ may be identified as imperfect annealing: that is, a small amount of the TG form is present. Here, the order of the stability of the conformation may be supposed to be: GG>TG>TT.

The treatment was also extended to discuss the species of $n=2$ and 3. On the molecular species of $n=2$ and 3, the results are nearly the same as in the case of $n=1$. That is, if these three forms coexist in the species of $n=1$, the six forms now considered for the $n=2$ and 3 species are fully acceptable. However, we cannot give any more detailed descriptions on the basis of only the data thus for obtained.

Model Compounds. The C–H stretching, CH₃ deformation, C–S stretching, and skeletal deformation vibrations are reproduced well by this set. For the CH₂ deformation vibrations, on the species of $n=1$, one each of the CH₂ bending, CH₂ wagging, CH₂ twisting, and CH₂ rocking vibrations are expected for each form. These four bands are fairly well reproduced by the calculations. In the cases of the $n=2$ and 3 species, the separation widths between or among the same methylene deformation bands are not so well reproduced. However, in general the transferability of the force constants is very good.

PTM and PTM-D2. The calculated data of PTM and PTM-D2 are listed in Tables 8 and 9, along with the observed data. A part of the Raman and infrared data of PTM which were obtained by Hendra et al.[17] are also listed. It is shown that the calculated frequencies agree satisfactorily well with the observed frequencies. It is also shown that the transferability

TABLE 8. OBSERVED AND CALCULATED FREQUENCIES (cm⁻¹), AND POTENTIAL ENERGY DISTRIBUTION, PED, OF PTM

Species	Obsd[a]	Calcd	PED[b]
A₁	1373[c]	1406	BCH₂
	1180[c]	1129	TCH₂
	648[c]	614	νC–S, BSCS
	335[c]	331	BCSC, BSCS
	—	78	τC–S
	—	2	BSCS, BCSC
A₂	1225	1188	WCH₂
	742	805	RCH₂
	735	724	νC–S
	—	99	τC–S
E	1368	1406	BCH₂
	1173	1187	WCH₂
	1155	1129	TCH₂
	882	821	RCH₂
	708	723	νC–S
	671	624	νC–S, BSCS
	355[c]	343	BCSC, BSCS
	—	177	BSCS, BCSC
	—	90	τC–S
	—	27	τC–S

The region above 1500 cm⁻¹ is omitted.
a) From Table 1.   b) Notations are the same as in Table 5.   c) From Ref. 17.

TABLE 9. OBSERVED AND CALCULATED FREQUENCIES (cm⁻¹), AND POTENTIAL ENERGY DISTRIBUTION, PED, OF PTM-D2

Species	Obsd[a]	Calcd	PED[b]
A₁	—	1032	BCD₂
	—	808	TCD₂
	—	583	νC–S
	—	325	BCSC, BSCS
	—	42	τC–S
	—	2	BSCS, BCSC
A₂	962	924	WCD₂, νC–S
	697	696	νC–S
	635	618	RCD₂
	—	105	τC–S
E	1012	1031	BCD₂
	908	926	WCD₂, νC–S
	885	808	TCD₂
	648	686	νC–S, RCD₂
	752	654	RCD₂, νC–S
	603	587	νC–S
	—	318	BSCS, BCSC
	—	160	BCSC, BSCS
	—	66	τC–S
	—	42	τC–S

The region above 1100 cm⁻¹ is omitted.
a) From Table 1.   b) Notations are the same as in Table 5.

of the force constants used on the model compounds is very good. The vibrations in relation to the methylene group shifted directly upon deuteration. The observed shifts correspond well with those expected.

Frequency-phase Difference Curves

It has been seen[13] that the observed CH₂ deformation frequencies of the CH₃S(CH₂S)$_n$CH₃ ($n=1-3$) series have some regularities between the degree of n and their fundamentals. Table 10 shows the observed frequencies of the model compounds and PTM in the methylene deformation region. The CH₂ bending or twisting band of PTM is at nearly the same frequency as that of the central bands of the $n=3$ species. On the other hand, the wagging and rocking bands of PTM lie outside of the bands of the $n=3$ species. These will be explained more quantitatively in the following section.

From the concept of the frequency-phase difference,[21] when the degree of n and the molecular conformation are confirmed, the infrared-active bands of the species become easily recognizable. On the species of $-(CH_2S)_n-$, the number of atoms per polymer unit is four; the vibrational degrees of freedom, therefore, are $3\times4=12$. The phase-difference, δ_a, is defined thus: $\delta_a=(a-1)\pi/n$ (a$=1$, 2, 3, ..., n), where n denotes the degree of polymerization. The species of $n=1$ correspond to CH₃SCH₂SCH₃; $n=2$, to CH₃SCH₂SCH₂SCH₃, and $n=3$, to CH₃SCH₂SCH₂SCH₂SCH₃. Figure 3 shows the frequency-phase difference curves in relation to the CH₂ deformation modes. The curves show the [G]-type frequency-phase dif-

TABLE 10. INFRARED FREQUENCIES (cm^{-1}) OF METHYLENE DEFORMATION VIBRATIONS OF $CH_3S(CH_2S)_nCH_3$ ($n=1-3$) AND PTM OBSERVED IN THE SOLID STATE

	$n=1$	$n=2$	$n=3$	PTM
$B CH_2$			1379	
		1381		
	1388[a]		1369	1368
		1372		
			1355	
$W CH_2$			1220	1225
		1219		
	1214[a]		1204	
		1193		
			1182	1173
$T CH_2$			1173	
		1167		
	1166		1153	1155
		1133		
			1126	
$R CH_2$			866	882
		844		
	808		811	
		780		
			760	742

a) Average of the doublet-band.
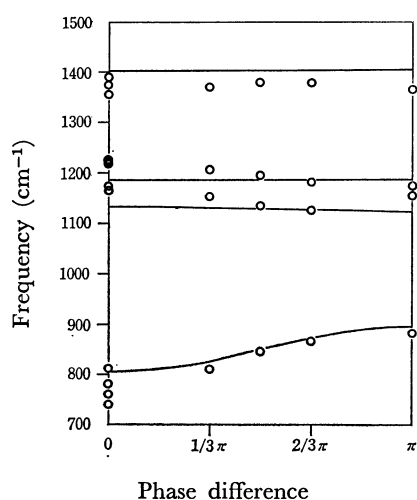
Fig. 3. Frequency-phase difference curves for the CH_2 bending, wagging, twisting, and rocking modes.

ference of PTM, and the plots are the observed ones. From this figure, the observed plots can be seen to correspond well with the calculated ones. The separation width of the observed CH_2 deformation bands can also be explained well by these curves. The tendency of the frequency-phase difference curve is conspicuous in the CH_2 rocking vibrations. For the [T]-type frequency-phase difference, detailed investigations have previously been made on polyethylene,[22] for example. The [T]-type frequency-phase difference curve is different from that of the [G] type. This is also conspicuous in the CH_2 rocking vibrations. In

the [T] type, the frequency change due to phase difference is less than that of the [G] type. It is natural that the curves of the PTM resemble those of the hexagonal POM; the frequencies themselves are very different, though. Since the CH_2 deformation frequencies of the molecular species of $n=1-3$ are explained well by the [G]-type curves, it is also confirmed that these model molecules exist in the [G] form in the solid state. This shows also that the force fields in PTM and its model compounds are nearly the same, and that, in the determination of the force fields of polymers, it is important to determine the force fields of their model compounds.

Discussion

The regularities lying between the degree of n and the CH_2 deformation frequencies are reasonably explained by the frequency-phase difference curves. The relations lying between n and the terminal methyl deformation frequencies do not appear very clearly in the calculated frequencies. That is, the calculated frequencies of the CH_3 degenerate deformation, the CH_3 symmetrical deformation, and the CH_3 rocking vibrations are around 1440, 1317, and 990—970 cm^{-1}. In the observed frequencies, very interesting results were obtained. For the CH_3 symmetrical deformation in the annealed spectra, the separation widths of the two bands are 28, 14, 6, and 21 cm^{-1} for the $n=0$, $n=1$, 2, and 3 species respectively. For the CH_3 rocking vibrations, the separations of the side bands are 129, 43, 14, and 17 cm^{-1} respectively in the above-mentioned species. That is, the separation width between side bands rapidly decreases from the $n=0$ to $n=2$ species, and then increases a little. As has previously been described, the stable conformation of these molecules is the [G] form. The skeletal form of these compounds is shown in Fig. 4. Two methyl groups of the $n=1$ species stand at the same edge, and the methylene group stands at the opposite position. Therefore, the interactions between the methyl and methylene groups are small. In the case of the $n=2$ species, things are the same in the $n=1$ species. In the species of $n=3$, the distance between the methyl groups at both ends becomes large. However, the central methylene and two methyl groups are on the same side, and the interactions among these groups become large. In the potential energy distribution, PED, or in the L-matrix, however, this tend-
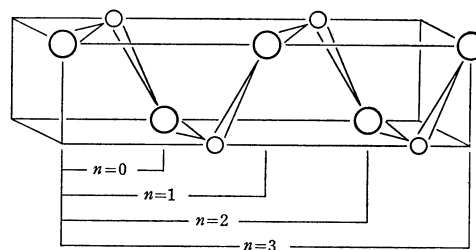

Fig. 4. Skeletal structures of $CH_3S(CH_2S)_nCH_3$ ($n=0-3$).
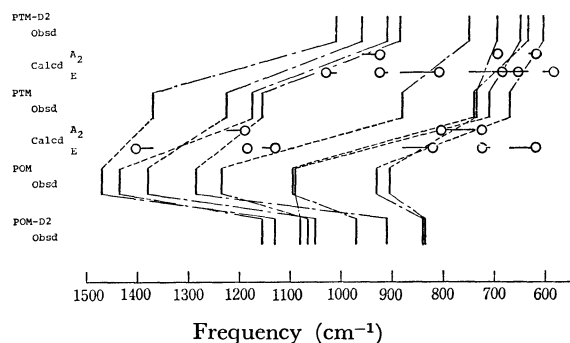Large circle: methyl or methylene group. Small circle: sulfur atom.

Fig. 5. Observed and calculated frequencies of PTM and PTM-D2, and obserbed frequencies of POM and POM-D2.

ency does not appear so clearly.

The vibrational spectra between PTM and POM will be briefly compared here. Figure 5 shows the observed frequencies of PTM, PTM-D2, POM, and POM-D2, along with the calculated frequencies of PTM and PTM-D2. The assignments of the observed bands of POM and POM-D2 have been made by several authors.[1,4,5] In this figure, the data obtained by Tadokoro et al.[1] are cited. The CH_2 bending, CH_2 wagging, and CH_2 twisting vibrations of PTM appear at frequencies lower by ca. 150—300 cm^{-1} than those of POM. In the case of the CH_2 rocking vibrations, the bands of PTM are much lower than the corresponding POM bands. However, the separation widths of the bands correspond well with PTM and POM. The stretching bands of PTM appear in a different spectral region from those of POM. The frequency shifts upon deuteration show nearly the same tendency.

The force constants of PTM may now be compared with the constants of POM, which are listed in Table 3 of Ref. 1. The set of No. 17 is used for comparison. The constants of PTM are much smaller than the corresponding constants of POM. The smaller values of the stretching constants show the weaker binding forces. The bending and repulsion constants, except for the constant of $F(HCH)$, are also much smaller than the corresponding constants of POM. From these results it is seen that the binding forces in PTM are much weaker than those in POM, and that the interatomic interacitons in PTM are smaller than those in POM.

For the $CH_3O(CH_2O)_nCH_3$ ($n=1$—5) species, the stable conformation in the solid state is confirmed to be the [G] form; in the liquid state the [G] form may also persist.[6,7] In the same way, it may be concluded that the conformation of the sulfur analogs is the [G] form in the solid state. In the liquid state, the [G] form may persist. On the other hand, n-alkane and poly-ethylene[23] exist in the [T] form. Moreover, in the cases of normal alkyl ethers[24] and normal alkyl sulfides,[25-27] the skeletal conformation is confirmed to be the [T] form. In the cases of n-alkane and polyethylene, the lone-pair electrons are not involved. For n-ethers and n-sulfides, the directions of the lone pairs on the oxygen or sulfur atoms coincide with those of the C–H

bonds of n-alkane and polyethylene. The present author has previously described[27] that the sulfur atom with lone-pair electrons can be regarded as a CH_2 group in the conformational analyses of alkyl sulfides. In the case of PTM, the molecular conformations of the [T] and [G] forms are shown below. In the case
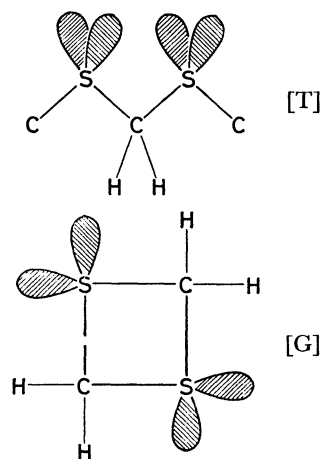
of the [G] form, the lone-pair electrons are coordinated in the center of the C–H bond directions. On the other hand, in the case of the [T] form, the lone-pair electrons on the sulfur atoms are in the same directions and the repulsion forces between lone pairs become large (rabbit-ear effect);[28] in consequence the [G] form may be stable. In the species of alkyl disulfides, sulfur atoms combine with each other. Therefore, the lone pairs on the sulfur atoms produce a powerful effect on the structure of these molecules. In conclusion, these molecules easily have a form which has almost a rectangle (e.g., the internal angle of ca. 85° has been proposed for dimethyl disulfide[29]). Therefore, the analysis of the conformation has been done with reference to the concept of the lone pairs.

Conclusion

The results for the infrared spectra of PTM and PTM-D2, and the normal coordinates of $CH_3S(CH_2S)_n$-CH_3 ($n=1$—3), PTM, and PTM-D2 reveal that the molecular form and the force fields of the model compounds fit well with those of PTM. On the molecular form in the solid state, the model compounds and PTM are confirmed to be the [G] form. On the molecular species of $n=1$, three forms are confirmed to exist in the liquid or gaseous state: GG, TG, and TT. On the species of $n=2$ and 3, many of the forms may coexist in the liquid or gaseous state. A comparison of the force fields between PTM and POM reveals that, in PTM, the intramolecular binding forces and non-bonded interatomic interactions are much weaker than those in POM.

References

1) H. Tadokoro, M. Kobayashi, Y. Kawaguchi, A. Kobayashi, and S. Murahashi, *J. Chem. Phys.*, **38**, 703 (1963).

2) V. Zamboni and G. Zerbi, *J. Polym. Sci.*, **C7**, 153 (1964).

3) H. Sugeta and T. Miyazawa, *Rept. Prog. Polym. Phys. Japan*, **9**, 177 (1966).

4) G. Zerbi and P. J. Hendra, *J. Mol. Spectrosc.*, **27**, 17 (1968).

5) H. Sugeta, T. Miyazawa, and T. Kajiura, *J. Polym. Sci.*, **B7**, 251 (1969).

6) H. Sugeta, H. Murata, and T. Miyazawa, The Annual Meeting of the Chemical Society of Japan, 16th, p. 373 (1963); 17th, p. 514 (1964); 18th, p. 467 (1965).

7) H. Sugeta, M. Ito, and T. Miyazawa, The 21st Annual Meeting of the Chemical Society of Japan, Vol. 1, p. 325 (1968).

8) G. Carazzolo, *J. Polym. Sci.*, *A*-1, **1**, 1573 (1963).

9) G. Carazzolo and G. Valle, *ibid.*, *A*-1, **3**, 4013 (1965).

10) G. Carazzolo and G. Valle, *Makromol. Chem.*, **90**, 66 (1966).

11) T. Uchida and T. Tadokoro, *J. Polym. Sci.*, *A*-2, **5**, 63 (1967).

12) Y. Shiro, M. Ohsaku, M. Hayashi, and H. Murata, This Bulletin, **43**, 609 (1970).

13) M. Ohsaku, Y. Shiro, and H. Murata, *ibid.*, **45**, 113 (1972).

14) M. Schmidt, K. Blaettner, P. Kochendörfer, and H. Ruf, *Z. Naturforsch.*, **21b**, 622 (1966).

15) J. B. Lando and V. Stannet, *J. Polym. Sci.*. **B2**, 375 (1964).

16) E. Gipstein, E. Wellisch, and O. J. Sweeting, *ibid.*, **B1**, 237 (1963).

17) P. J. Hendra, D. S. Watson, and M. Mammi, *Spectrochim. Acta*, **28A**, 351 (1972).

18) M. Hayashi, Y. Shiro, and H. Murata, This Bulletin, **39**, 1857 (1966).

19) M. Hayashi, Y. Shiro, T. Osima, and H. Murata, *ibid.*, **38**, 1734 (1965).

20) M. Ohsaku, Y. Shiro, and H. Murata, *ibid.*, **45**, 3035 (1972).

21) T. Miyazawa, *Nippon Kagaku Zasshi*, **88**, 111 (1967).

22) M. Tasumi, T. Shimanouchi, and T. Miyazawa, *J. Mol. Spectrosc.*, **9**, 261 (1962); **11**, 422 (1963).

23) R. G. Snyder, *J. Chem. Phys.*, **47**, 1316 (1967).

24) R. G. Snyder and G. Zerbi, *Spectrochim. Acta*, **23A**, 391 (1967).

25) D. W. Scott and M. Z. El-Sabban, *J. Mol. Spectrosc.*, **30**, 317 (1969).

26) M. Ohsaku, Y. Shiro, and H. Murata, This Bulletin, **46**, 1399 (1973).

27) M. Ohsaku, to be published.

28) R. O. Hutchins, L. O. Kopp, and E. L. Eliel, *J. Amer. Chem. Soc.*, **90**, 7174 (1968); M. Ōki and H. Nakanishi, This Bulletin, **45**, 3419 (1971).

29) D. Sutter, H. Dreizler, and H. D. Rudolph, *Z. Naturforsch.*, **20a**, 1676 (1965).